Proteomic Profiling of Human Melanoma Metastatic Cell Line Secretomes

ARTICLE *in* JOURNAL OF PROTEOME RESEARCH · AUGUST 2011

Impact Factor: 4.25 · DOI: 10.1021/pr200511f · Source: PubMed

Journal of proteome research

ARTICLE

pubs.acs.org/jpr

Proteomic Profiling of Human Melanoma Metastatic Cell Line Secretomes

Micaela Rocco,[†,‡] Livia Malorni,[§,‡] Rosaria Cozzolino,[§] Giuseppe Palmieri,[∥] Carla Rozzo,[∥] Antonella Manca,[∥] Augusto Parente,[†] and Angela Chambery[†,*]

[†]Department of Life Sciences, Via Vivaldi 43, Second University of Naples, I-81100 Caserta, Italy

[§]Proteomic and Biomolecular Mass Spectrometry Center, Institute of Food Science and Technology, National Research Council (CNR), Via Roma 64, I-83100 Avellino, Italy

[∥]Unit of Cancer Genetics, Institute of Biomolecular Chemistry, National Research Council (CNR), Traversa La Crucca 3, Baldinca Li Punti, I-07100 Sassari, Italy

Supporting Information

ABSTRACT: During the last few years, the incidence and mortality of human melanoma have rapidly increased. Metastatic spread of malignant melanoma is often associated with cancer progression with poor prognosis and survival. These processes are controlled by dynamic interactions between tumor melanocytes and neighboring stromal cells, whose deregulation leads to the acquisition of cell proliferation capabilities and invasiveness. It is increasingly clear that a key role in carcinogenesis is played by secreted molecules either by tumor and surrounding stromal cells. To address the issue of the proteins secreted during cancer progression, the proteomic profiling of secretomes of cancer cell lines from different melanoma metastases of the same patient (PE-MEL-41, PE-MEL-47, and PE-MEL-43) was performed by applying a shotgun LC−MS/MS-based approach. The results provide a list of candidate proteins associated with the metastatic potential of PE-MEL melanoma cell lines. Among them, several matricellular proteins previously reported as involved in melanoma aggressiveness were identified (i.e., SPARC, osteopontin). In addition, the extracellular matrix protein 1 that stimulates proliferation and angiogenesis of endothelial cells as well as the fibronectin, involved in cell adhesion and motility, were identified. The present work provides the basis to clarify the complex extracellular protein networks implicated in human melanoma cell invasion, migration, and motility.

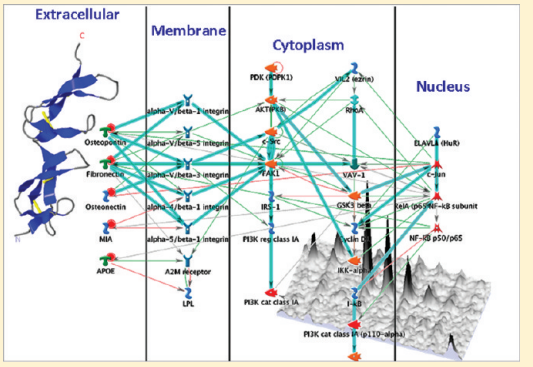

KEYWORDS: melanoma, metastasis, LC−MS, proteomic profiling, secretome

INTRODUCTION

Cancer progression requires a coordinated and dynamic multicellular behavior regulated by signals integrated through the tissue microenvironment.[1] In this process, cell−cell and cell−microenvironment interactions are critical determinants for tumor development, growth and dissemination.[2] Indeed, the ability of neoplastic cells to recruit support from neighboring stromal cells is essential for their survival.[3] Furthermore, the mutual interaction between malignant cells and vascular, immune and inflammatory systems also plays a significant role in carcinogenesis.[4] Emerging evidence support the hypothesis that microenvironment composition is a critical determinant of cancer suppression or progression.[4]

The complex network of cell−cell interactions is mediated by soluble factors released by cells into the extracellular environment, including a plethora of bioactive molecules influencing cell's functions and phenotype (e.g., proteinases, extracellular matrix proteins, growth factors, cytokines and chemokines). The secreted molecules, referred as cell "secretome", mediate the intercellular interactions by inducing paracrine and autocrine signaling that participate in the maintenance of cellular homeostasis. To identify novel biomarkers, new avenues of investigation have been focused on the characterization of secreted proteins from cancer cell lines and neoplastic tissues (cancer secretomics).[5−8]

Secreted proteins thus constitute an important class of molecules that determine, regulate and coordinate many biological processes in multicellular organisms including growth, proliferation and differentiation at the cellular level. Furthermore, extracellular proteins also regulate development, immune defense, blood coagulation and tumorigenesis at the level of tissues and organisms.[2] In addition, the microenvironment surrounding the primary tumors is regarded to be also a major regulator of metastases, the primary cause of mortality in most cancer pathologies.[9] The multistage process of cancer metastasis involve sequential molecular events that confer to cancer cells the ability to escape from the primary tumor, disseminate, survive, seed and grow at distant sites.[10] The understanding of the molecular basis

Received: May 30, 2011

of cancer metastases represents an attractive perspective for translating basic research to the clinical tools for cancer treatment. Although new insights at the gene level enhanced our understanding of the metastatic process, the nature of the changes of secreted proteins accompanying the metastatic process remains elusive. In spite of the increasing number of studies on cancer secretomics, few pioneering works report the metastasis-related differential secretome characterization. Xue and coworkers reports the differential secretome analysis of colorectal cancer metastasis.[11] To this aim, the secretome of a primary colorectal cancer cell line (SW480) was compared with that of a lymph node metastatic subline (SW620) from the same disease by shotgun proteomic analysis. Among the differentially expressed proteins, trefoil factor 3 and growth/differentiation factor 15 (GDF15) were identified as potential biomarkers for the prediction of colorectal cancer metastasis. Similarly, the identification of secreted proteins related to the acquisition of the aggressive phenotype of the bladder cancer cell line T24 was performed by 2D electrophoresis coupled to MALDI-TOF MS and LC−MS/MS.[12] Several extracellular proteins were identified, including secreted protein acidic cysteine-rich (SPARC), for which strong evidence suggest a role in bladder cancer cell motility and invasiveness. Recently, the cancer secretome research opens new prespectives into the pathogenic mechanisms of melanoma, a malignant tumor of melanocytes whose incidence has been increasing during the last 10 years (Source: National Cancer Institute, SEER Program). The high interest in melanoma research is also related to the high mortality rate of patients due to the metastatic potential of primary melanoma. A comprehensive study of melanoma secretome pattern has been performed by Paulitschke et co-workers.[13] To this aim, a comparison between the human M24met melanoma cell line and normal melanocyte secretomes and cytoplasmic fractions was performed by applying a shotgun LC−MS/MS approach. In addition, the associated stroma cells (i.e., normal human fibroblasts and melanoma-associated fibroblasts from mouse xenografts) were also characterized. More recently, the B16 mouse melanoma model has been investigated for the characterization of the secreted proteins involved in melanoma metastatic dissemination.[14] However, to our knowledge, no proteomic studies have been reported on secretome analysis of human melanoma primary tumors and their associated metastatic potential.

In this study, we investigated the secretome profiles of human metastatic cell lines by applying a shotgun LC−MS/MS-based approach. To study this process, we took advantage of three melanoma cell lines (PE-MEL-41, PE-MEL-47, and PE-MEL-43), isolated from different metastases of the same patient, which have been reported as a suitable model system for the study of melanoma aggressiveness.[15] Moreover, a comprehensive genetic and molecular analysis was also performed to provide a complementary characterization of the gene alterations underlying the differential metastatic behavior of PE-MEL cell lines.

EXPERIMENTAL SECTION

PE-MEL Cell Lines

The PE-MEL-41, PE-MEL-43, and PE-MEL-47 (formerly named as PES-41, PES-43, and PES-47) cell lines were isolated from different melanoma metastases of the same patient undergoing surgery with curative intent: PE-MEL-41 from a locoregional skin metastasis, PE-MEL-47 from a distant subcutaneous metastasis, and PE-MEL-43 from a visceral (lung) metastasis as previously reported.[15] Cell lines were cultured in Dulbecco's modified Eagle's medium (DMEM, Invitrogen, Carlsband, CA) supplemented with 10% FCS (FBS, Hyclone, Logan, UT), 2 mM L-glutamine (GIBCO), 100 U/mL penicillin G and 0.1 mg/mL streptomycin (GIBCO). Cells were maintained at 37 °C in humidified air containing 5% CO_2. Cells were routinely passaged weekly and the medium was changed every two days.

For the secretome analysis, PE-MEL-41/43/47 cells (2.5×10^6) were seeded in 30 cm plates in complete DMEM/10% FBS for 24 h. Culture media were then replaced with DMEM containing 0.5% FCS for 24 h, washed extensively with PBS 1× and serum-starved for 24 h before conditioned media collection performed from two culture preparations to address biological variation. The number of living and dead cells has been determined by trypan blue staining, as previously described.[16] For cell count and viability assays PE-MEL-41/43/47 cells were dissociated with trypsin solution 10x (Sigma-Aldrich, St. Louis, MO). For the viable count, cell suspension was diluted 1:10 in 0.25% trypan blue solution, incubated for 2 min and counted using a Burker chamber. Cell concentration and cell viability were determined on the basis of the total cell count, the dilution factor and the trypan blue dye exclusion. Data validation by Western Blot analysis was performed on an additional, independent, biological replicate.

Genetic and Molecular Analyses

For mutation analysis, genomic DNA was amplified and PCR products were directly sequenced using an automated fluorescence-cycle sequencer (ABIPRISM 3130, Applied Biosystems, Foster City, CA), as previously described.[17] Immunocytochemical analysis was performed on cultured melanoma cells, following standard procedures and using primary monoclonal antibodies against $p16^{CDKN2A}$ (JC-2 Lab Vision-Neo-Markers, Fremont, CA) as well as pRB and $pERK_{1-2}$ (Santa Cruz Biotechnology, Santa Cruz, CA) proteins. Intensity and distribution of cellular immunostaining was used to classify gene expression as follow: strongly positive (+++), moderately positive (++), weakly positive (+) or negative (−). Finally, fluorescence in situ hybridization (FISH) was performed using probes specific for candidate gene loci (*Cyclin D1/CCND1, MITF, EGFR, cKIT*), following previously described procedures.[18]

Sample Preparation and Tryptic Digestion

Conditioned media were collected, lyophilized and resuspended in 1 mL of 25 mM NH_4HCO_3. The proteins were then precipitated with 20% trichloroacetic acid for 30 min on ice and centrifuged for 15 min at 14 000 rpm. Pellets were washed with diethyl ether and acetone, air-dried and resuspended in 50 μL of 25 mM NH_4HCO_3. Samples were thoroughly sonicated into an ultrasonic bath for 10−15 min. Protein samples were reduced with 2.5 mM DTT at 60 °C for 30 min and carbamidomethylated with 7.5 mM iodoacetamide at room temperature in the dark for 30 min. Enzymatic hydrolyses were performed by two subsequent additions (3 and 16 h at 37 °C) of 5 μL of a TPCK-treated trypsin solution (6 ng/μL) to the reduced and alkylated mixtures as previously described.[19,20] After digestion, samples were dried under vacuum in a SpeedVac Vacuum (Savant Instruments, Holbrook, NY), resuspended in 20 μL of 0.1% formic acid (FA) and centrifuged at 14 000 rpm for 15 min. Aliquots of the supernatant (6 μL) were analyzed by LC−MS/MS. All analyses were conducted in duplicate.

dx.doi.org/10.1021/pr200511f | J. Proteome Res. XXXX, XXX, 000–000

LC−MS Configurations

Mass spectrometry analysis was performed using a quadrupole time-of-flight mass spectrometer equipped with an electrospray ionization source (ESI Q-TOF MS, Waters S.p.A, Manchester, UK). Tryptic peptides were separated by means of a modular CapLC system (Waters, Manchester, UK) as reported elsewhere.[20] Samples were loaded onto a C18 precolumn (5 mm length × 300 μm ID) at a flow rate of 20 μL/min and desalted for 5 min with a solution of 0.1% formic acid. Peptides were then directed onto a symmetry-C18 analytical column (10 cm × 300 μm ID) using 5% CH_3CN, containing 0.1% formic acid at a flow rate of 5 μL/min. The elution was obtained by increasing the CH_3CN/0.1% formic acid concentration from 5 to 55% over 60 min. The precursor ion masses and associated fragment ion spectra of the tryptic peptides were mass measured with the mass spectrometer directly coupled to the chromatographic system. The TOF analyzer of the mass spectrometer was externally calibrated with a multipoint calibration using selected fragment ions that resulted from the collision-induced decomposition (CID) of human [Glu1]-fibrinopeptide B [500 fmol/μL in CH_3CN/H_2O (50:50), 0.1% formic acid] at an infusion rate of 5 μL/min in the TOF MS/MS mode. The instrument resolution in MS/MS mode for the [Glu1]-fibrinopeptide B fragment ion at m/z 684.3469 was found to be above 5000 FWHM (full width at half-maximum).

Electrospray mass spectra and tandem MS/MS data were acquired on the Q-TOF mass spectrometer operating in the positive ion mode with a source temperature of 80 °C and with a potential of 3500 V applied to the capillary probe. MS/MS data on tryptic peptides were acquired in the data directed analysis (DDA) MS/MS mode, automatically switching between MS and MS/MS acquisition for the three most abundant ion peaks per MS spectrum. Charge state recognition was used to select doubly- and triply charged precursor ions for the MS/MS experiments, which also includes the automated selection of the collision energy based on both charge and mass. A maximum of three precursor masses was defined for concurrent MS/MS acquisition from a single MS survey scan. MS/MS fragmentation spectra were collected from m/z 50 to 1600.

Data Processing and Protein Identification

For spectra processing raw data were centroided, deisotoped, and charge-state-reduced to produce a single, accurately measured monoisotopic mass for each peptide and the associated fragment ions.

Mascot Distiller software (version 2.3.2.0, Matrix Science) was used to generate peak lists from raw data files. When generating these peak lists, grouping of spectra was performed with a maximum intermediate retention time of 30 s and maximum intermediate scan count of 1. Grouping was done with 0.3 Da tolerance on the precursor ion. A peak list was only generated when the MS/MS spectrum contained more than 10 peaks and the relative S/N limit was set at 2. MS/MS peak lists were searched with Mascot using the Mascot Distiller search tool interface (Matrix Science). Only peptides that were ranked one and scored above the identity threshold score ($p < 0.05$) were selected. For protein identifications, processed peak lists were searched against the uniprot_sprot database with *Homo sapiens* as taxonomy restriction (release 2011_02; 20 254 entries). Trypsin endoprotease was selected for cleavage specificity allowing one missed cleavage site. *S*-carbamidomethyl derivative of cysteine and oxidation of methionine were specified in Mascot as fixed and variable modifications, respectively. Database search was performed by using a mass tolerance of 100 ppm and a fragment ion tolerance of 0.6 Da. Identifications were accepted as positive when probability scores were significant at $p < 0.05$. A validation for MS/MS searches was performed according to the method of Elias and Gygi, 2007 by performing searches against a decoy *Homo sapiens* database.[21] Briefly, during the search, every time a protein sequence from the target database was tested, a random sequence of the same length was automatically generated and tested using a significance threshold of 0.05. For the MS/MS validation, using the peptide matches above identity threshold as scoring system, the FDR for PE-MEL-41, PE-MEL-43, and PE-MEL-47 samples were estimated at 4.8, 2.5 and 3.1%, respectively. For representative MS/MS spectra, fragmentation pattern were manually double checked to verify sequence assignments by means of the Biolynx application of MassLynx 4.0 software (Waters, Manchester, U.K.). Comparative LC−MS/MS data analysis was also performed by using the MSight software,[22] freely available from the Swiss Institute of Bioinformatics (www.expasy.org/Msight). To this end, data files (.RAW) generated using MassLynx Software (Waters, Manchester, U.K.) were imported into MSight following conversion to mzXML files.

Expression Analysis

For Western blot analysis, proteins were resolved by 12% SDS-PAGE under reducing conditions and transferred onto nitrocellulose membrane (Sartorius, Göttingen, Germany) with an electroblot apparatus (Bio-Rad, Milan, Italy), according to the manufacturer's instructions. The membrane was blocked with 5% milk in TTBS (0.1% Tween-20 in TBS, w/v) for 1 h at room temperature and washed three times with TTBS. Subsequently, membranes were incubated with primary antibodies (Santa Cruz Biotechnology, Santa Cruz, CA) diluted in 5% milk in TTBS overnight at 4 °C. In particular, the following dilutions were used: anti-SPARC, 1:1000 (1.B.790: sc-73051); anti-ECM1, 1:500 (P-19: sc65087); anti-OPN, 1:500 (ZZ09: sc 80262). Membranes were then washed with TTBS, incubated with the appropriate HRP-conjugated secondary antibody diluted 1:5000 in 2% milk in TTBS for 1 h at room temperature. Immunoreactive protein bands were visualized by the enhanced chemiluminescence (ECL) Plus Western Blotting Detection System (GE Healthcare, Buckinghamshire, UK) according to the manufacturer's instructions. For *in vivo* expression analysis of candidate proteins, immunohistochemistry (IHC) was performed on 3−4 μm sections of formalin-fixed, paraffin-embedded tissues from metastases of melanoma patients, using standard procedures. Immunodetection was obtained with the same antibodies used in Western blot analysis.

Bioinformatics Analyses

Significantly enriched categories for identified proteins were related to biological functions using the Ingenuity Pathways Analysis (IPA) software, version 6.3 (Ingenuity Systems, http://www.ingenuity.com). The lists of proteins were imported into the IPA platform for batch analysis as previously reported.[23,24]

Identified proteins were analyzed for secretion pathways according to SecretomeP 2.0 Server[25] (http://www.cbs.dtu.dk/services/SecretomeP/). If the neural network exceeded or was equal to a value of 0.50 (NN-score ≥0.50), but no signal peptide was predicted, protein is considered to be potentially secreted via a non-classical pathway. Those proteins with a predicted N-terminal signal sequence were confirmed using SignalP 3.0,[26] available at http://www.cbs.dtu.dk/services/SignalP/ (set for

dx.doi.org/10.1021/pr200511f | J. Proteome Res. XXXX, XXX, 000–000

Table 1. Genetic and Molecular Analysis Carried Out on the PE-MEL Human Melanoma Cell Lines[a]

	ICC			FISH (gene/control ≥2)				mutation analysis				
cell line *derived from*	pRB	pERK	p16	*CCND1*	*MITF*	*EGFR*	*cKIT*	*BRAF*	*NRAS*	$p16^{CDKN2A}$	*TP53*	*PTEN*
PE-MEL-41 *Loco-regional subcutaneous nodule*	+	+	+	0	30%	0	0	V600E	0	W110*+A148T	0	Del./Rear. exons 2−5
PE-MEL-47 *Distant subcutaneous nodule*	++	+	−	60%	50%	20%	0	V600E	0	W110*+A148T	0	Del./Rear. exons 2−5
PE-MEL-43 *Lung nodule*	++	+++	−	30%	30%	20%	0	V600E	0	W110*+A148T	0	Del./Rear. exons 2−5

[a] ICC, immunocytochemistry; FISH, fluorescence *in situ* hybridization; Del./Rear., deletions/rearrangements.

eukaryotes using both neural networks and hidden Markov models). These proteins were considered to be secreted via a classical pathway (endoplasmic reticulum/Golgi-dependent pathway). Finally, TMHMM 2.0 server (http://www.cbs.dtu.dk/services/TMHMM/) was used to predict the occurrence of α-helical transmembrane domains.[27]

Network Analysis Using MetaCore

MetaCore (GeneGo, St. Joseph, MI) was used to map the identified proteins into biological networks. MetaCore is an integrated software suite for functional analysis of experimental data. It is based on a proprietary manually curated database of human protein−protein, protein−DNA, and protein−compound interactions. In addition, metabolic and signaling pathways and the effects of bioactive molecules are also included in the analysis. Identified proteins were converted into gene symbols and uploaded into MetaCore platform for network analysis using the shortest path algorithm.[28]

RESULTS

PE-MEL human cell lines are derived from three different melanoma metastases and have been already described for the expression levels and activity of the CXCR4 receptor, the most widely expressed chemokine receptor among cancers.[15] To evaluate the existence of putative differences in their malignant phenotype, all three PE-MEL cell lines underwent detailed genetic and molecular analysis, focusing on gene and pathways already demonstrated to play a key role in melanoma pathogenesis.[29]

All three cell lines were mutated in *BRAF* (V600E; the most common mutation described for this gene) and $p16^{CDKN2A}$ (W110*+A148T; the first variant is a nonsense mutation causing the production of a truncated protein, whereas the latter one has been classified as a sequence variation of unknown functional significance) genes (Table 1). No point mutation was found in *PTEN* and *TP53* genes, whereas genomic deletions and/or rearrangements of exons 2 to 5 in *PTEN* gene were observed in all three PE-MEL cell lines (Table 1). Detection of a wild type *NRAS* gene confirmed literature data reporting that *BRAF* and *NRAS* mutations are mutually exclusive[30,31] (Table 1). All detected mutations have been previously reported in the Human Gene Mutation Database (http://archive.uwcm.ac.uk).

The immunocytochemical analyses show that the PE-MEL-43 cell line presented the highest expression levels of activated pERK protein (ERK is downstream the RAS-BRAF-MEK signal transduction cascade and its activation through phosphorylation induces cell proliferation;[29,30] Table 1, Figure 1A). A reduced (PE-MEL-41, Figure 1C) or absent (PE-MEL-47 and PE-MEL-43, Figure 1D) expression of the $p16^{CDKN2A}$ protein was found

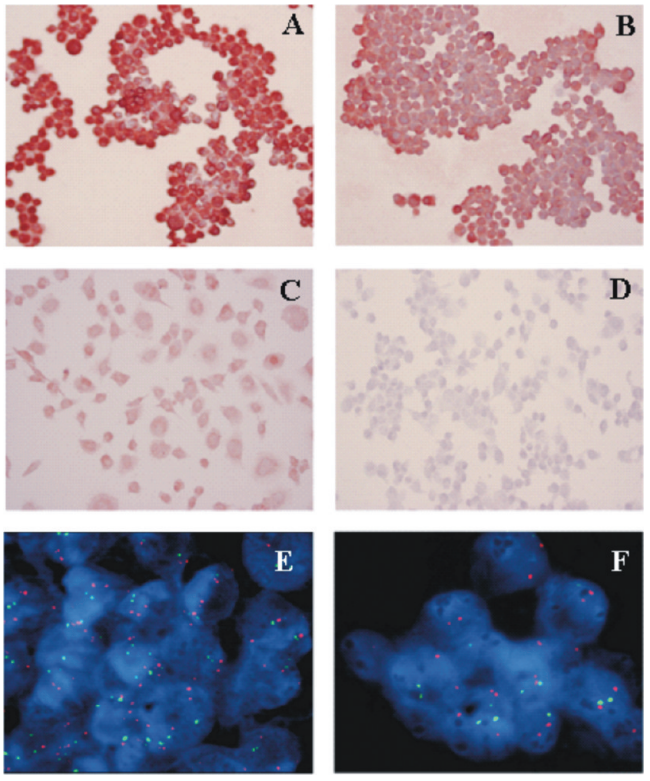

Figure 1. Representative results of immunocytochemistry and FISH analysis on melanoma cell lines. (A−D) From intensively positive (+++) to negative (−) cell staining (A, pERK in PE-MEL-43; B, pRB in PE-MEL-43; C, p16 in PE-MEL-41; D, p16 in PE-MEL-43). (E−F) FISH analysis showing gene amplification (E, *MITF* in PE-MEL-47) or normal disomy (F, *CCND1* in PE-MEL-41).

in our series, whereas increasing levels of phosphorylated RB (pRB) protein was observed moving from cells derived from loco-regional metastasis (PE-MEL-41) to cells derived from distant secondary lesions (PE-MEL-47 and PE-MEL-43, Table 1 and Figure 1B). On this regard, the $p16^{CDKN2A}$ protein acts as a proliferation inhibitor by binding the CDK4/6 kinases and blocking phosphorylation of the RB protein, which lead cells to cycle arrest.[30,31] Therefore, the coexistence of down-regulation or inactivation of the $p16^{CDKN2A}$ gene and hyper-phosphorylation of the RB protein has been demonstrated to strongly induce cell proliferation and increase aggressiveness of transformed melanocytic cells. FISH analysis revealed that all three cell lines were quite similarly amplified in *MITF* gene locus (Figure 1E) as expected, since this gene has been reported to be amplified during melanoma progression.[32] Furthermore, all cell lines were

dx.doi.org/10.1021/pr200511f |J. Proteome Res. XXXX, XXX, 000–000

Table 2. Proteins Identified by Shot-Gun LC−MS/MS in the Secretomes of PE-MEL-41, PE-MEL-43, and PE-MEL-47 Cell Lines[a]

		PE-MEL-41			PE-MEL-43			PE-MEL-47				
accession	protein name	score[b]	peptides[c]	rms error	score	peptides	rms error	score	peptides	rms error	secretome P[d]	signal P[e]
Q9HAP3	Fibronectin (FN1)	573	36 (19)	83	391	27 (14)	44	204	16 (5)	74	0.35	Signal (1.0)
P09486	SPARC/Osteonectin	310	9 (6)	91	243	14 (5)	43	349	13 (8)	77	0.94	Signal (1.0)
Q99988	Growth/differentiation factor 15 (GDF15)	125	2 (2)	94	39	2 (1)	56	184	4 (2)	75	0.88	Signal (1.0)
P60709	Actin, cytoplasmic 1 (ACTB)	64	4 (2)	93	63	2 (1)	41	97	5 (3)	70	0.50	
Q16610	Extracellular matrix protein 1 (ECM1)	48	2 (1)	86	61	6 (2)	44	108	5 (2)	81	0.62	
P02649	Apolipoprotein E (APOE)	**25**	1	76	37	5 (1)	47	146	7 (3)	72	0.88	Signal (1.0)
P02768	Serum albumin (ALB)	37	3 (2)	86	54	1 (1)	47	53	2 (1)	77	0.47	Signal (1.0)
P07093	Glia-derived nexin (GDN, Serpine2)	**19**	2	89	43	4 (1)	31	**17**	1 (1)	67	0.47	
O15240	Neurosecretory protein (VGF)	154	12 (5)	82	n.d.	n.d.	n.d.	n.d.	n.d.	n.d.	0.32	Signal (1.0)
P18065	Insulin-like growth factor-binding protein 2 (IGFBP2)	54	2 (1)	65	76	5 (2)	43	n.d.	n.d.	n.d.	0.79	
P61769	Beta-2-microglobulin (B2M)	30	1 (1)	80	n.d.	n.d.	n.d.	n.d.	n.d.	n.d.	0.91	Signal (1.0)
P02765	Alpha-2-HS-glycoprotein	28	1 (1)	91	n.d.	n.d.	n.d.	n.d.	n.d.	n.d.	0.54	Signal (1.0)
P01011	Alpha-1-antichymotrypsin	n.d.	n.d.	n.d.	66	4 (2)	37	n.d.	n.d.	n.d.	0.64	
Q16674	Melanoma-derived growth regulatory protein (MIA)	n.d.	n.d.	n.d.	32	1 (1)	57	n.d.	n.d.	n.d.	0.84	Signal (1.0)
P62937	Peptidyl-prolyl cis−trans isomerase A (PPIA)	n.d.	n.d.	n.d.	30	3 (1)	37	n.d.	n.d.	n.d.	0.34	
P25391	Laminin subunit alpha-1	n.d.	n.d.	n.d.	29	1 (1)	50	n.d.	n.d.	n.d.	0.38	Signal (1.0)
P04406	Glyceraldehyde-3-phosphate dehydrogenase (GAPDH)	n.d.	n.d.	n.d.	30	2 (1)	33	41	2 (1)	62	0.46	
P10451	Osteopontin (SPP1)	n.d.	n.d.	n.d.	68	2 (1)	54	30	5 (1)	73	0.65	Signal (1.0)
Q08380	Galectin-3-binding protein (LGALS3BP)	n.d.	n.d.	n.d.	65	5 (2)	38	71	5 (2)	78	0.56	
Q16769	Glutaminyl-peptide cyclotransferase (QPCT, POR)	n.d.	n.d.	n.d.	**18**	2	49	66	2 (1)	81	0.60	
P08670	Vimentin (VIM)	n.d.	n.d.	n.d.	73	4 (1)	40	37	3 (1)	68	0.51	
P14618	Pyruvate kinase isozymes M1/M2 (PKM2)	n.d.	n.d.	n.d.	n.d.	n.d.	n.d.	48	2 (1)	80	0.44	
Q9BXX0	Emilin-2	n.d.	n.d.	n.d.	n.d.	n.d.	n.d.	32	1 (1)	73	0.33	

[a] Number of matched peptides and the mean error in ppm are reported along with the Mascot probability score values. Additional experimental details for MS identifications are reported in Supplementary Table 2S of Supporting Information. Single based-peptide identifications details are reported in Supplementary Table 3S of Supporting Information. n.d. not detected. [b] Significant Mascot protein scores ($p < 0.05$). Scores below the significant threshold (in bold) have been reported only for proteins significantly detected in at least another condition. [c] Total number of peptide matches to a protein. The number of unique peptides with an ion score above the significant threshold ($p < 0.05$) is reported in parentheses. [d] Secretion prediction according to SecretomeP server. Proteins with NN-score ≥0.5 are predicted as secreted by nonclassical secretory pathways. [e] Secretion prediction according to SignalP server. Numbers in parentheses indicate the signal peptide probability.

found to be disomic at *cKIT* gene locus, previously reported to be amplified in mucosal melanomas.[30] In addition, no amplification of *Cyclin D1* (*CCND1*) and *EGFR* genes (which are associated with increasing CDK activity and activation of the RAS-BRAF-MEK pathway) was detected in PE-MEL-41 (Figure 1F), while these loci were amplified in cells derived from distant metastases (i.e., PE-MEL-47 and PE-MEL-43) .

Overall, our findings clearly indicate that, although all three cell lines are genetically altered in the major genes (*BRAF*, $p16^{CDKN2A}$, and *PTEN*), PE-MEL-43 and PE-MEL-47 present a more malignant tumor phenotype (with the highest aggressiveness showed by PE-MEL-43 cells) as compared with that of the PE-MEL-41 cell line.

However, besides molecular and genetic factors intrinsic to cancer cells, tumor progression and metastasis formation also depend on stimuli and factors from the microenvironment, including but not limited to growth factors, cellular adhesion molecules, extracellular matrix proteins and secreted proteins (e.g., proteases, chemokines etc.).

To investigate the secretome of PE-MEL cell lines, the proteomic profiling of conditioned media of PE-MEL-41, PE-MEL-43, and PE-MEL-47 cell lines was performed by applying a shot-gun LC−MS/MS approach. To this end, cell viability of PE-MEL cell lines was evaluated to compare unstarved and starved culture conditions. Results show that starvation did not affect cell viability in the three cell lines, thus minimizing the possibility of

dx.doi.org/10.1021/pr200511f |J. Proteome Res. XXXX, XXX, 000–000

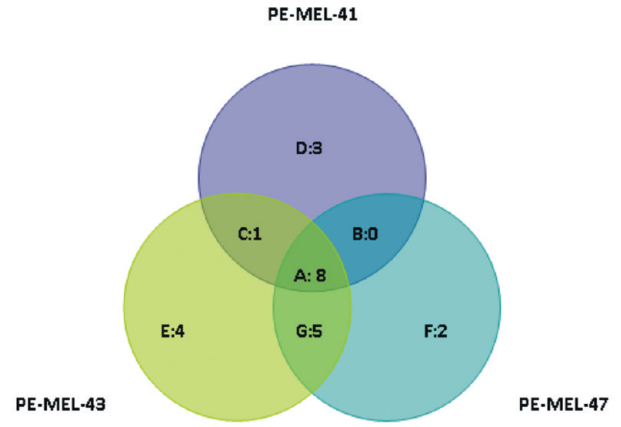

A
Fibronectin
SPARC
Growth/differentiation factor 15
Actin, cytoplasmic 1
Extracellular matrix protein 1
Apolipoprotein E
Serum albumin
Glia-derived nexin

C
Insulin-like growth factor-binding protein 2

D
Neurosecretory protein VGF
Beta-2-microglobulin
Alpha-2-HS-glycoprotein

E
Alpha-1-antichymotrypsin
Melanoma-derived growth regulatory protein
Peptidyl-prolyl cis-trans isomerase A
Laminin subunit alpha-1

F
Pyruvate kinase isozymes M1/M2
Emilin-2

G
Glyceraldehyde-3-phosphate dehydrogenase
Osteopontin
Galectin-3-binding protein
Glutaminyl-peptide cyclotransferase
Vimentin

Figure 2. Venn diagrams of proteins identified by shot-gun LC−MS/MS analysis in the conditioned media of PE-MEL-41, PE-MEL-43, and PE-MEL-47 cell lines.

potential contamination of the conditioned medium by intracellular proteins occurring following cell lysis and death events (Supplementary Table 1S, Supporting Information). Therefore, conditioned media of the three cell lines were collected following serum starvation and proteins were subjected to tryptic digestion and LC−MS/MS analysis as described in the Methods section. Data were filtered by considering only protein identifications with significant probability scores ($p < 0.05$). By tandem mass spectrometry and Mascot database search, 23 non-redundant proteins were identified in the secretomes of PE-MEL cell lines (Table 2). Additional experimental details for MS identifications are reported in Supplementary Table 2S of Supporting Information. According to the MIAPE guidelines, single based-peptide identifications details and fragmentation spectra are reported in Supplementary Table 3S and Supplementary Figures 1S−24S of Supporting Information. The Venn diagram reported in Figure 2 shows a qualitative comparison of proteins identified in PE-MEL-41, PE-MEL-43, and PE-MEL-47 secretomes. A set of 8 proteins was commonly detected in the three cell line conditioned media, including Fibronectin and SPARC/Osteonectin, both identified with a high number of peptides. Representative extracted ion chromatograms for the doubly charged precursor ion at m/z 608.37 identified to SPARC (Mascot Ions Score: 61, Expect value: 2.8e-05) are reported in Figure 3A. The three-dimensional view of regions corresponding to peak elution in the LC−MS run analyzed with MSight software are reported in Figure 3B.

A qualitative cross-section analysis revealed that 3, 4, and 2 proteins were uniquely detected in the PE-MEL-41, PE-MEL-43, and PE-MEL-47 samples, respectively (Figure 2). Only 1 protein (i.e., Insulin-like growth factor-binding protein 2) was commonly detected in PE-MEL-41 and PE-MEL-43 and no proteins were found to be common to PE-MEL-41 and PE-MEL-47 secretomes. This finding is in line with the differences observed in tumor phenotype between the two PE-MEL cell lines.

Proteins secretion in the extracellular space occurs at least by three physiological mechanisms, including classical and nonclassical secretion pathways. In the classical secretion pathway, the N-terminal signal peptide is responsible for the secretion while, for the nonclassical pathways, the signal sequence is missing and proteins are released by endosomal recycling, translocation across membranes, exosomes and other unknown processes.[33,34] Therefore, we analyzed the identified proteins for signal peptide driven secretion and unconventional secretion pathways by using the SignalP 3.0 and SecretomeP 2.0 prediction servers (Table 2). These analyses revealed that approximately 78% (18/23) of the identified proteins were predicted to be secreted. Among them, 11 proteins (∼48%) were predicted to have a signal peptide, thus suggesting a secretion following the classical endoplasmic reticulum/Golgi dependent pathway. On the other hand, 7 proteins (∼30%) were predicted to be released from cells by mammalian nonclassical secretion mechanisms (NN-score ≥ 0.5). According to the TMHMM server, one protein was classified as an integral membrane protein, corresponding to Melanoma-derived growth regulatory protein, a growth factor secreted by malignant melanoma cell lines.

Significantly enriched categories for identified proteins were related to biological functions using IPA software (Figure 4). A significant number of proteins was involved in cancer pathologies, cell death processes, cellular growth and proliferation. In addition, the enriched biological functions also included proteins related to cancer metastasis, cellular movement and adhesion of eukaryotic cells. Interestingly, five proteins (i.e., Fibronectin, FN1; Growth/differentiation factor 15, GDF15; SPARC/osteonectin; Osteopontin, SPP1; Vimentin, VIM) were related to the invasion of tumor cell lines (see Discussion).

dx.doi.org/10.1021/pr200511f |J. Proteome Res. XXXX, XXX, 000–000

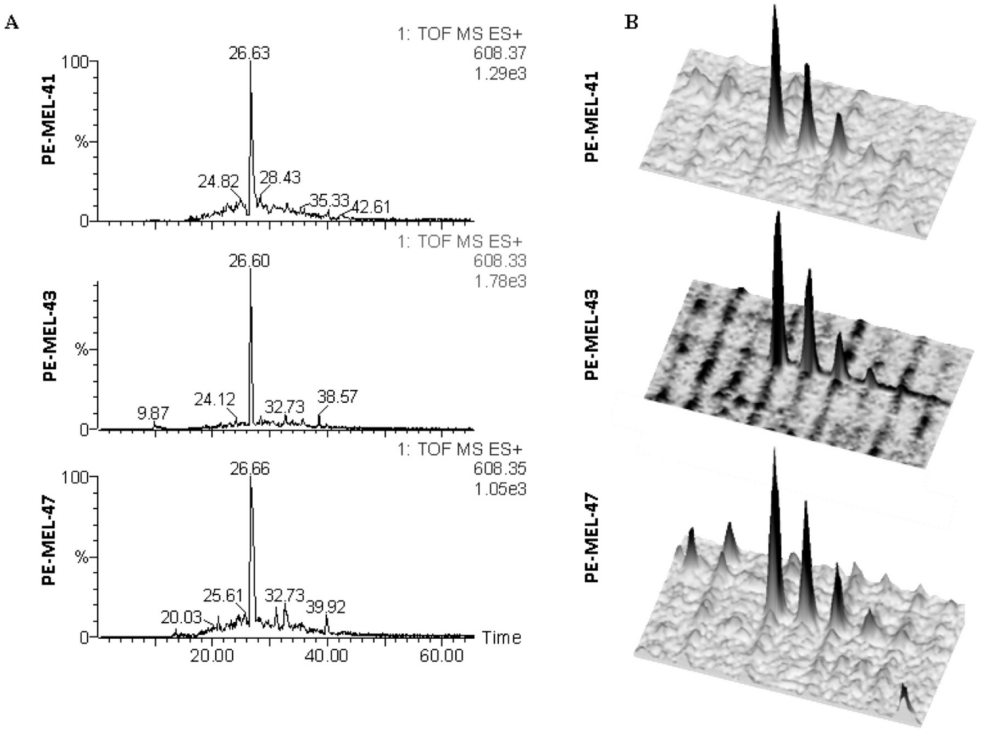

Figure 3. (A) Extracted ion chromatograms for the doubly charged precursor ion at m/z 608.37 identified to SPARC. (B) 3D view of regions corresponding to the m/z 608.37 peak elution in the LC−MS runs.

Therefore, two out of three proteins related to tumor cell line invasion (SPARC/osteonectin and Osteopontin) were selected for further validation by Western blot analysis performed on conditioned media of PE-MEL cell lines (Figure 5A). In addition, Extracellular matrix protein 1 (ECM1) expression, preferentially expressed by metastatic epithelial tumors and reported to be involved in cell proliferation and angiogenesis,[35,36] was also analyzed by Western blot (Figure 5C). As expected on the basis of the proteomic results, SPARC/osteonectin and ECM1 were confirmed to be secreted in the three PE-MEL cell lines, even under unstarved conditions (data not shown). On the other hand, Osteopontin was demonstrated to be secreted in PE-MEL-43 and PE-MEL-47 but not in PE-MEL-41 cell lines (Figure 5B). The expression of SPARC/osteonectin and Osteopontin has also been evaluated by immunohistochemistry (IHC) in a subset of available tissue sections of melanoma metastases (i.e., 2 subcutaneous lesions and 2 affected lymph nodes) from different patients. In Figure 6, representative examples of IHC staining for the two proteins are shown. Altogether, a diffusely moderate expression of SPARC/osteonectin and, in contrast, a very weak immunostaining (with few poorly positive cells per field areas at the microscope) for Osteopontin were observed in all four metastatic tumor samples.

To investigate the potential involvement of the identified secreted proteins in the activation of known molecular pathways, a network map was constructed using the Metacore software. A specific subset of secreted proteins was mapped on a network converging on Focal adhesion kinase (FAK), a protein tyrosine kinase found in cell-matrix attachment sites (focal adhesions) activated on integrin-ligand binding (Figure 7). Indeed, the core molecules of this network were found to include, at the level of the plasma membrane, members of the alpha-V/beta integrins family. Among secreted proteins mapped on the FAK network, three proteins (i.e., Apolipoprotein E, SPARC/osteonectin and Fibronectin) were found in the conditioned media of all PE-MEL cell lines. On the contrary, Osteopontin was detected in the secretomes of PE-MEL-43 and PE-MEL-47 samples and Melanoma-derived growth regulatory protein was uniquely identified in the PE-MEL-43 secretome.

DISCUSSION

Tumor metastasis is a dynamic process regulated by complex interactions occurring between tumor and host cells. Three major steps in this cascade of sequential events lead to tumor metastasis: (i) individual tumor cells detach from the primary tumor; (ii) tumor cells infiltrate into the surrounding stroma and, through the vasculature or lymphatic systems, are carried to distant sites; (iii) the tumor cells leave the vasculature and invade the target organ. Tumor cells with high metastatic potential are able to complete these processes, thus acquiring an aggressive phenotype.[4]

Malignant melanoma, due to the well-described sequential progression of the disease, constitutes an excellent model to study the molecular changes occurring during cellular transformation processes. Indeed, proliferation within the radial growth phase of normal melanocytes leads to benign melanocytic nevi (i.e., dysplastic nevi).[37] When the lesions enter the vertical growth phase, the repertoire of adhesion molecules changes, allowing the tumor to invade the dermis, thus acquiring the ability to metastasize. Metastatic spread of malignant melanoma is often associated with cancer progression with poor prognosis and survival.[37]

These processes are finely regulated by mutual interactions between tumor melanocytes and neighboring stromal cells, whose deregulation leads to the acquisition of cell proliferation capabilities and invasiveness. It is increasingly clear that a key role in carcinogenesis is played by secreted molecules either by tumor and surrounding stromal cells.[5] Intensive research activities have

dx.doi.org/10.1021/pr200511f |J. Proteome Res. XXXX, XXX, 000–000

A

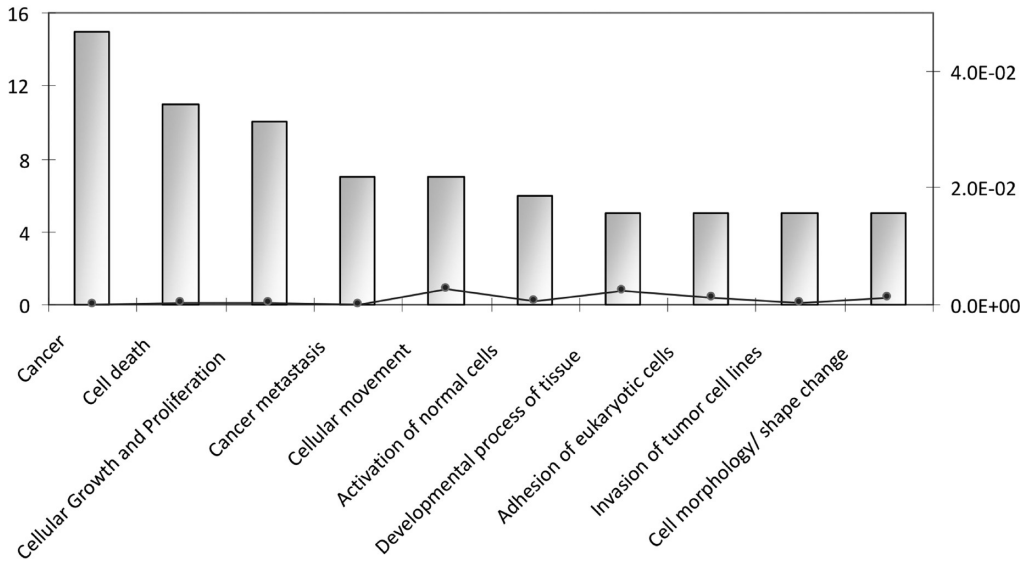

B

Biological Function	p-value	Molecules	No. molecules
Cancer	1.54E-06	ACTB, ALB, APOE, B2M, ECM1, FN1, GAPDH, GDF15, LGALS3BP, PKM2, QPCT, SERPINE2, SPARC, SPP1, VIM	15
Cell death	2.44E-04	ALB, APOE, B2M, FN1, GAPDH, GDF15, LGALS3BP, PKM2, SERPINE2, SPARC, SPP1	11
Cellular Growth and Proliferation	1.67E-04	ALB, B2M, ECM1, FN1, GDF15, PKM2, POR, SERPINE2, SPARC, SPP1	10
Cancer metastasis	3.04E-07	ACTB, APOE, FN1, GDF15, QPCT, SPP1, VIM	7
Cellular movement	2.81E-03	ALB, APOE, FN1, GDF15, SERPINE2, SPARC, S PP1	7
Activation of normal cells	6.00E-04	ACTB, APOE, B2M, FN1, SPP1, VIM	6
Developmental process of tissue	2.42E-03	ECM1, FN1, PKM2, SPARC, SPP1	5
Adhesion of eukaryotic cells	1.12E-03	ACTB, APOE, FN1, LGALS3BP, SPP1	5
Invasion of tumor cell lines	2.11E-04	FN1, GDF15, SPARC, SPP1, VIM	5
Cell morphology/ shape change	1.31E-03	ALB, APOE, FN1, SPARC, SPP1	5

Figure 4. (A) Bar chart of the significantly enriched biological functions of proteins secreted by PE-MEL cell lines; (B) *p*-values and the molecules mapped on the enriched categories. ACTB, Actin; ALB, Albumin; APOE, Apolipoprotein E; B2M, Beta-2-microglobulin; ECM1, Extracellular matrix protein 1; FN1, Fibronectin; GAPDH, Glyceraldehyde-3-phosphate dehydrogenase; GDF15, Growth/differentiation factor 15; LGALS3BP, Galectin-3-binding protein, PKM2, Pyruvate kinase isozymes M1/M2; POR, QPCT, Glutaminyl-peptide cyclotransferase; SERPINE2, Glia-derived nexin; SPARC, secreted protein acidic cysteine-rich (osteonectin); SPP1, Osteopontin; VIM, Vimentin.

been focused on searching serum prognostic markers, either mRNA or proteins, correlated to melanoma aggressiveness.[38] Recently, the murine melanoma B16 model was used to study different grades of melanoma aggressiveness by analyzing secreted proteins by a proteomic approach.[14]

In this work, the secretomes of human metastatic cell lines were analyzed by applying a shotgun LC−MS/MS with the aim to profile proteins secreted by human primary tumors, potentially involved in the acquisition of the aggressive phenotype. For this purpose, three cell lines established from different metastases of the same patient were used to obtain a representation of distinct malignant phenotypes: among the two cell lines derived from subcutaneous metastases, PE-MEL-47 showed molecular features indicating higher aggressiveness in comparison to its parental PE-MEL-41 cell line, and PE-MEL-43 derived from a visceral metastasis presented an even higher aggressive phenotype when compared to the other two cell lines (see Table 1). Accordingly, the results of the PE-MEL secretome analysis provide a list of candidates potentially associated with the metastatic properties of PE-MEL human melanoma cell lines. Among them, proteins involved in biological processes closely related to cancer metastasis including cell proliferation and apoptosis, cell adhesion, cellular movement, and ECM-interaction were identified. Several proteins known to be involved in tissue remodeling and tumor invasion were commonly detected in the three cell lines. These include the adhesion protein ECM1, which stimulates the proliferation and angiogenesis of endothelial cells,[35,36,39] and the protease inhibitor Glial-derived nexin (GDN), a serine protease inhibitor known to potently and irreversibly inhibit several proteases, including thrombin, urokinase plasminogen activator and tissue plasminogen activator.[40] Recently, it has been reported that GDN is a substrate for Matrix metalloproteinase-9, a key enzyme for the proteolytic degradation of extracellular matrix during tumor invasion and metastasis.[41] Another protein commonly identified in PE-MEL-41, PE-MEL-43, and PE-MEL-47 secretomes was Growth/differentiation factor 15 (GDF15), also called Macrophage Inhibitory Cytokine-1 (MIC-1), a member of the transforming growth factor-beta superfamily, whose deregulation has been associated with cancer progression in various human diseases, including melanoma.[42,43] GDF15 is involved in pleiotropic functions including growth inhibition, apoptosis induction, cell detachment, and pro-invasiveness.[44] Moreover, a potential application of GDF15 in the evaluation of colorectal

dx.doi.org/10.1021/pr200511f |*J. Proteome Res.* XXXX, XXX, 000–000

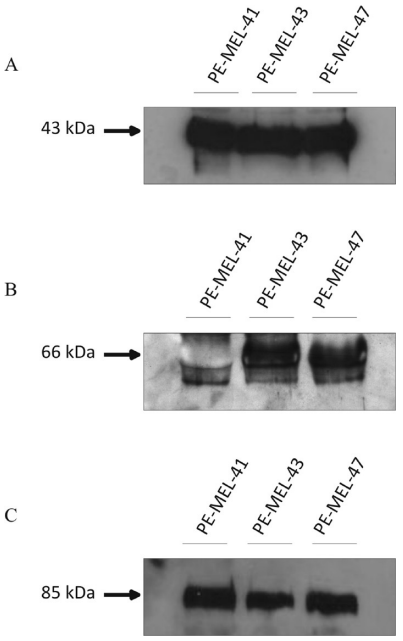

Figure 5. Validation of selected identified proteins by Western blot. TCA-precipitated conditioned media collected from PE-MEL-41, PE-MEL-43, and PE-MEL-47 cell lines were analyzed for the expression levels and secretion of (A) SPARC/Osteonectin, (B) Osteopontin and (C) Extracellular matrix protein 1.

cancer lymph node metastasis has been also suggested.[11] Additional proteins previously reported to be implicated with cancer aggressiveness, metastatic potential and shorter survival in different types of malignancies included the pyruvate kinase M1/M2 (PKM2), being the M2 isoform a plasma tumor marker for melanoma.[45]

Among proteins uniquely detected in PE-MEL-43 secretome, Melanoma-derived growth regulatory protein (MIA) was identified. This protein is not secreted by normal melanocytes, but it was reported to be strongly expressed by advanced primary and metastatic melanomas.[43] Interestingly, MIA serum levels were correlated with clinical tumor progression in melanoma patients.[46]

Several matricellular proteins previously reported as involved in melanoma aggressiveness and implicated in cancer progression were identified, including Galectin-3-binding protein (LGALS3BP). An active role in enhancing tumorigenicity, stimulating tumor cell migration *in vitro* and metastasis *in vivo* was previously reported for LGALS3BP.[47,48] Furthermore, LGALS3BP stimulated interleukin-6 by involving the activation of the ERK1/2 pathway in neuroblastoma cells.[47] LGALS3BP was detected in PE-MEL-43 and PE-MEL-47 but not in PE-MEL-41 secretomes. Another ECM protein previously correlated with the acquisition of invasive and metastatic behavior of melanoma cells was Fibronectin (FN1), involved in cell adhesion and motility. As for LGALS3BP, also the synthesis of FN1 was stimulated by ERK/MAP kinase by upregulating the transcription factor early growth response-1 (Egr-1), indicating that self-production of FN1 may play a role in melanoma tumorigenesis.[49] Furthermore, high FN1 levels were found in melanoma cells presenting the oncogenic *BRAF* mutations.[49] These findings highly correlate with the common identification of FN1 in the secretomes of PE-MEL-41, PE-MEL-43, and PE-MEL-47 cell lines, all carrying the *BRAF* mutation.

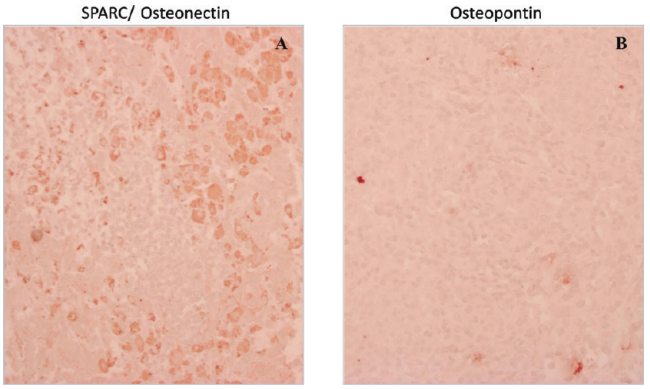

Figure 6. Immunohistochemical staining of (A) SPARC/Osteonectin and (B) Osteopontin in melanoma metastases.

Besides FN1, two other matricellular proteins, SPARC (also known as osteonectin) and osteopontin (OPN) were identified. SPARC is a glycoprotein involved in cell-ECM interactions that clinically correlates with aggressiveness of melanomas and the acquisition of metastatic phenotypes.[50−52] Accordingly, SPARC was detected in all PE-MEL cell lines with comparable expression levels as confirmed by Western blot analysis. Besides its role in regulating EMC-interactions, SPARC is a counter-adhesive molecule that induces the epithelial−mesenchymal transition, thus contributing to transformation of melanocytes to melanoma.[51] High levels of SPARC in melanoma, pancreatic cancer, gliomas and thyroid cancer have been associated with poor prognosis.[53] SPARC also suppresses the expression of E-cadherin, whose loss is responsible for the progression from the radial-growth phase to the vertical-growth phase of melanoma and increases phosphorylation of focal adhesion kinase.[54] These findings suggest that SPARC modulate cell-ECM interactions and promote an invasive melanoma phenotype.[55] In addition, SPARC overexpressing melanoma cells showed upregulation of OPN a secreted adhesive glycoprotein involved in the regulation of inflammation, tissue remodeling, and cell survival.[56] OPN interacts with receptors, such as integrins, via arginine−glycine−aspartate (RGD)- and non-RGD containing adhesive domains, thus mediating cell-matrix interactions and cellular signaling.[57] It has been reported that OPN up-regulates the migratory activity of B16 melanoma cells in a MAPK/ERK dependent manner.[58] Recently, substantial evidence has linked OPN expression to the regulation of metastatic spread of tumor cells.[59] In particular, OPN expression has been related to melanoma development and progression.[60−63] Accordingly, in our experimental system, OPN was only detected in PE-MEL-43 and PE-MEL-47 cell lines. This finding was further validated by Western blot analysis. These results are very interesting also considering that OPN was previously suggested as a prognostic marker of melanoma progression and invasion.[63] Moreover, it has been reported that the major receptor for OPN in mouse melanocytes was the $\alpha v\beta 3$ integrin, suggesting that its autocrine production in transformed melanocytic cells may be a first step toward malignancy.[64] Although very preliminary *in vivo* data have been obtained in our series, SPARC protein seems to be more markedly and homogeneously expressed among metastatic melanomas in comparison to the OPN protein (see Figure 6). However, further studies on a larger collection of tissue samples from different anatomic sites of metastatic melanoma patients are awaited for a better characterization of their role as potential histopathological markers.

dx.doi.org/10.1021/pr200511f |*J. Proteome Res.* XXXX, XXX, 000–000

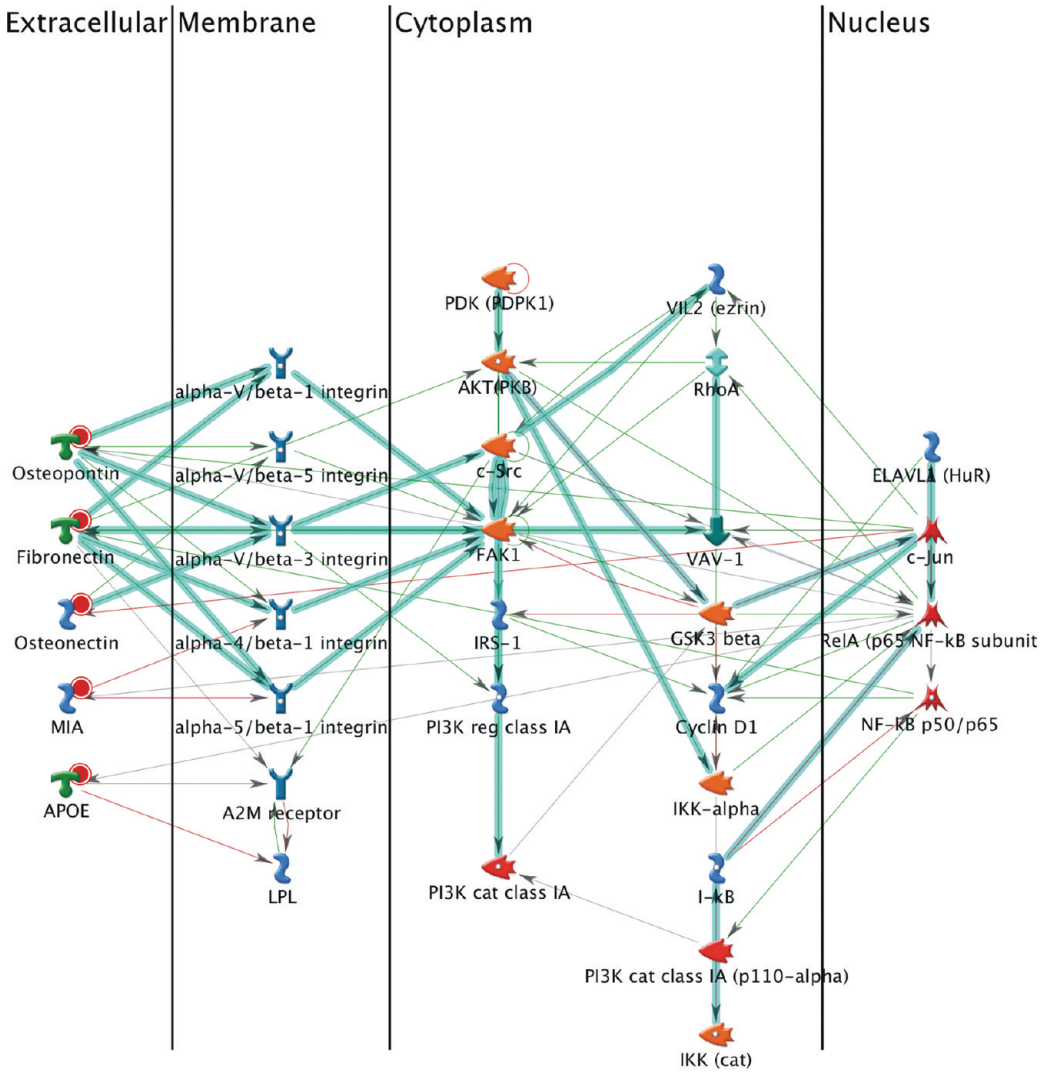

Figure 7. Network analysis of secreted proteins identified by LC−MS/MS for PE-MEL-41, PE-MEL-43, and PE-MEL-47 cell lines by MetaCore mapping tool. The network was generated using the shortest path algorithm to map interaction between the proteins. Nodes represent proteins; lines between the nodes indicate direct protein−protein interaction. The small red circle denotes the identified proteins.

The role of the cell surface integrins in melanoma progression is eliciting a growing interest, since many of them have been implicated in melanoma growth and metastasis.[65] Accordingly, specific subsets of proteins secreted by the PE-MEL cell lines were mapped on a functional network mainly converging, at plasma membrane level, on integrins $\alpha v\beta 1$, $\alpha v\beta 5$ and $\alpha v\beta 3$ (Figure 7). It has been reported that the integrin αv subunit is widely expressed in melanomas regardless of disease stage and the most notable pair relevant for melanoma metastasis is the $\alpha v\beta 3$ vitronectin receptor.[65] At the cytoplasm level, the core molecule of the identified network was found to be the focal adhesion kinase (FAK1), a nonreceptor protein tyrosine kinase found in cell-matrix attachment sites and activated on integrin-ligand binding.[66] FAK protein was up-regulated in all human melanoma cells, suggesting an involvement of FAK in the oncogenic mechanisms of melanomas accounting for the highly aggressive, anchorage independent phenotype of this tumor.[66,67]

Overall, the identified candidate proteins from cell lines with different malignant properties hold great promise to further investigate the mechanisms of melanoma cell motility and aggressiveness, as well as to serve as a source of potential disease biomarkers. Although further efforts are required to fully elucidate their biological functions in melanoma progression and metastasis, information derived from the analysis of the identified proteins may provide useful suggestions for clarifying the role of extracellular signals in cancer metastatic processes.

■ ASSOCIATED CONTENT

Supporting Information

Supplementary tables and figures. This material is available free of charge via the Internet at http://pubs.acs.org.

■ AUTHOR INFORMATION

Corresponding Author

*Mailing address: Department of Life Sciences, Second University of Naples Via Vivaldi 43 I-81100 Caserta, Italy. Phone: +39 0823 274535. Fax: +39 0823 274571. E-mail: angela.chambery@unina2.it.

dx.doi.org/10.1021/pr200511f |J. Proteome Res. XXXX, XXX, 000–000

Author Contributions

[‡]These authors contributed equally to this work

■ ACKNOWLEDGMENT

This study was supported by funds from the Second University of Naples and Sardinian Regional Government (Regione Autonoma Sardegna). We are grateful to Dr. Maria Cristina Sini for contributing to molecular analysis of melanoma cells. We thank Dr. Paolo Antonio Ascierto and his Melanoma Unit at National Cancer Institute "Pascale" of Naples for providing PE-MEL cell lines.

■ REFERENCES

(1) Hanahan, D.; Weinberg, R. A. The hallmarks of cancer. *Cell* **2000**, *100* (1), 57–70.

(2) Bissell, M. J.; Radisky, D. Putting tumours in context. *Nat. Rev. Cancer* **2001**, *1* (1), 46–54.

(3) Tlsty, T. D.; Hein, P. W. Know thy neighbor: stromal cells can contribute oncogenic signals. *Curr. Opin. Genet. Dev.* **2001**, *11* (1), 54–9.

(4) Langley, R. R.; Fidler, I. J. Tumor cell-organ microenvironment interactions in the pathogenesis of cancer metastasis. *Endocr. Rev.* **2007**, *28* (3), 297–321.

(5) Karagiannis, G. S.; Pavlou, M. P.; Diamandis, E. P. Cancer secretomics reveal pathophysiological pathways in cancer molecular oncology. *Mol. Oncol.* **2010**, *4* (6), 496–510.

(6) Pavlou, M. P.; Diamandis, E. P. The cancer cell secretome: a good source for discovering biomarkers? *J Proteomics* **2010**, *73* (10), 1896–906.

(7) Xue, H.; Lu, B.; Lai, M. The cancer secretome: a reservoir of biomarkers. *J. Transl. Med.* **2008**, *6*, 52.

(8) Makridakis, M.; Vlahou, A. Secretome proteomics for discovery of cancer biomarkers. *J. Proteomics* **2010**, *73* (12), 2291–305.

(9) Joyce, J. A.; Pollard, J. W. Microenvironmental regulation of metastasis. *Nat. Rev. Cancer* **2009**, *9* (4), 239–52.

(10) Nguyen, D. X.; Bos, P. D.; Massague, J. Metastasis: from dissemination to organ-specific colonization. *Nat. Rev. Cancer* **2009**, *9* (4), 274–84.

(11) Xue, H.; Lu, B.; Zhang, J.; Wu, M.; Huang, Q.; Wu, Q.; Sheng, H.; Wu, D.; Hu, J.; Lai, M. Identification of serum biomarkers for colorectal cancer metastasis using a differential secretome approach. *J. Proteome Res.* **2010**, *9* (1), 545–55.

(12) Makridakis, M.; Roubelakis, M. G.; Bitsika, V.; Dimuccio, V.; Samiotaki, M.; Kossida, S.; Panayotou, G.; Coleman, J.; Candiano, G.; Anagnou, N. P.; Vlahou, A. Analysis of secreted proteins for the study of bladder cancer cell aggressiveness. *J. Proteome Res.* **2010**, *9* (6), 3243–59.

(13) Paulitschke, V.; Kunstfeld, R.; Mohr, T.; Slany, A.; Micksche, M.; Drach, J.; Zielinski, C.; Pehamberger, H.; Gerner, C. Entering a new era of rational biomarker discovery for early detection of melanoma metastases: secretome analysis of associated stroma cells. *J. Proteome Res.* **2009**, *8* (5), 2501–10.

(14) Rondepierre, F.; Bouchon, B.; Bonnet, M.; Moins, N.; Chezal, J. M.; D'Incan, M.; Degoul, F. B16 melanoma secretomes and in vitro invasiveness: syntenin as an invasion modulator. *Melanoma Res.* **2010**, *20* (2), 77–84.

(15) Scala, S.; Giuliano, P.; Ascierto, P. A.; Ierano, C.; Franco, R.; Napolitano, M.; Ottaiano, A.; Lombardi, M. L.; Luongo, M.; Simeone, E.; Castiglia, D.; Mauro, F.; De Michele, I.; Calemma, R.; Botti, G.; Caraco, C.; Nicoletti, G.; Satriano, R. A.; Castello, G. Human melanoma metastases express functional CXCR4. *Clin. Cancer Res.* **2006**, *12* (8), 2427–33.

(16) Illuzzi, G.; Bernacchioni, C.; Aureli, M.; Prioni, S.; Frera, G.; Donati, C.; Valsecchi, M.; Chigorno, V.; Bruni, P.; Sonnino, S.; Prinetti, A. Sphingosine kinase mediates resistance to the synthetic retinoid N-(4-hydroxyphenyl)retinamide in human ovarian cancer cells. *J. Biol. Chem.* **2010**, *285* (24), 18594–602.

(17) Casula, M.; Muggiano, A.; Cossu, A.; Budroni, M.; Caraco, C.; Ascierto, P. A.; Pagani, E.; Stanganelli, I.; Canzanella, S.; Sini, M.; Palomba, G.; Palmieri, G. Role of key-regulator genes in melanoma susceptibility and pathogenesis among patients from South Italy. *BMC Cancer* **2009**, *9*, 352.

(18) Sini, M. C.; Manca, A.; Cossu, A.; Budroni, M.; Botti, G.; Ascierto, P. A.; Cremona, F.; Muggiano, A.; D'Atri, S.; Casula, M.; Baldinu, P.; Palomba, G.; Lissia, A.; Tanda, F.; Palmieri, G. Molecular alterations at chromosome 9p21 in melanocytic naevi and melanoma. *Br. J. Dermatol.* **2008**, *158* (2), 243–50.

(19) Chambery, A.; Vissers, J. P.; Langridge, J. I.; Lonardo, E.; Minchiotti, G.; Ruvo, M.; Parente, A. Qualitative and quantitative proteomic profiling of cripto(−/−) embryonic stem cells by means of accurate mass LC-MS analysis. *J. Proteome Res.* **2009**, *8* (2), 1047–58.

(20) Chambery, A.; Severino, V.; D'Aniello, A.; Parente, A. Precursor ion discovery on a hybrid quadrupole-time-of-flight mass spectrometer for gonadotropin-releasing hormone detection in complex biological mixtures. *Anal. Biochem.* **2008**, *374* (2), 335–45.

(21) Elias, J. E.; Gygi, S. P. Target-decoy search strategy for increased confidence in large-scale protein identifications by mass spectrometry. *Nat. Methods* **2007**, *4* (3), 207–14.

(22) Palagi, P. M.; Walther, D.; Quadroni, M.; Catherinet, S.; Burgess, J.; Zimmermann-Ivol, C. G.; Sanchez, J. C.; Binz, P. A.; Hochstrasser, D. F.; Appel, R. D. MSight: an image analysis software for liquid chromatography-mass spectrometry. *Proteomics* **2005**, *5* (9), 2381–4.

(23) Severino, V.; Chambery, A.; Vitiello, M.; Cantisani, M.; Galdiero, S.; Galdiero, M.; Malorni, L.; Di Maro, A.; Parente, A. Proteomic analysis of human U937 cell line activation mediated by Haemophilus influenzae type b P2 porin and its surface-exposed loop 7. *J. Proteome Res.* **2010**, *9* (2), 1050–62.

(24) Mendelsohn, B. A.; Malone, J. P.; Townsend, R.; Gitlin, J. Proteomic analysis of anoxia tolerance in the developing zebrafish embryo. *Comp. Biochem. Physiol., Part D* **2009**, *4* (1), 21–31.

(25) Bendtsen, J. D.; Jensen, L. J.; Blom, N.; Von Heijne, G.; Brunak, S. Feature-based prediction of non-classical and leaderless protein secretion. *Protein Eng. Des. Sel.* **2004**, *17* (4), 349–56.

(26) Bendtsen, J. D.; Nielsen, H.; von Heijne, G.; Brunak, S. Improved prediction of signal peptides: SignalP 3.0. *J. Mol. Biol.* **2004**, *340* (4), 783–95.

(27) Krogh, A.; Larsson, B.; von Heijne, G.; Sonnhammer, E. L. Predicting transmembrane protein topology with a hidden Markov model: application to complete genomes. *J. Mol. Biol.* **2001**, *305* (3), 567–80.

(28) Chen, R.; Brentnall, T. A.; Pan, S.; Cooke, K.; Moyes, K. W.; Lane, Z.; Crispin, D. A.; Goodlett, D. R.; Aebersold, R.; Bronner, M. P. Quantitative proteomics analysis reveals that proteins differentially expressed in chronic pancreatitis are also frequently involved in pancreatic cancer. *Mol. Cell. Proteomics* **2007**, *6* (8), 1331–42.

(29) Palmieri, G.; Capone, M.; Ascierto, M. L.; Gentilcore, G.; Stroncek, D. F.; Casula, M.; Sini, M. C.; Palla, M.; Mozzillo, N.; Ascierto, P. A. Main roads to melanoma. *J. Transl. Med.* **2009**, *7*, 86.

(30) Curtin, J. A.; Fridlyand, J.; Kageshita, T.; Patel, H. N.; Busam, K. J.; Kutzner, H.; Cho, K. H.; Aiba, S.; Brocker, E. B.; LeBoit, P. E.; Pinkel, D.; Bastian, B. C. Distinct sets of genetic alterations in melanoma. *N. Engl. J. Med.* **2005**, *353* (20), 2135–47.

(31) Palmieri, G.; Casula, M.; Sini, M. C.; Ascierto, P. A.; Cossu, A. Issues affecting molecular staging in the management of patients with melanoma. *J. Cell. Mol. Med.* **2007**, *11* (5), 1052–68.

(32) Garraway, L. A.; Widlund, H. R.; Rubin, M. A.; Getz, G.; Berger, A. J.; Ramaswamy, S.; Beroukhim, R.; Milner, D. A.; Granter, S. R.; Du, J.; Lee, C.; Wagner, S. N.; Li, C.; Golub, T. R.; Rimm, D. L.; Meyerson, M. L.; Fisher, D. E.; Sellers, W. R. Integrative genomic analyses identify MITF as a lineage survival oncogene amplified in malignant melanoma. *Nature* **2005**, *436* (7047), 117–22.

(33) Walter, P.; Gilmore, R.; Blobel, G. Protein translocation across the endoplasmic reticulum. *Cell* **1984**, *38* (1), 5–8.

(34) Mellman, I.; Warren, G. The road taken: past and future foundations of membrane traffic. *Cell* **2000**, *100* (1), 99–112.

(35) Wang, L.; Yu, J.; Ni, J.; Xu, X. M.; Wang, J.; Ning, H.; Pei, X. F.; Chen, J.; Yang, S.; Underhill, C. B.; Liu, L.; Liekens, J.; Merregaert, J.; Zhang, L. Extracellular matrix protein 1 (ECM1) is over-expressed in malignant epithelial tumors. *Cancer Lett.* **2003**, *200* (1), 57–67.

(36) Han, Z.; Ni, J.; Smits, P.; Underhill, C. B.; Xie, B.; Chen, Y.; Liu, N.; Tylzanowski, P.; Parmelee, D.; Feng, P.; Ding, I.; Gao, F.; Gentz, R.; Huylebroeck, D.; Merregaert, J.; Zhang, L. Extracellular matrix protein 1 (ECM1) has angiogenic properties and is expressed by breast tumor cells. *FASEB J.* **2001**, *15* (6), 988–94.

(37) Hearing, V.; Leong, S. *From Melanocytes to Melanoma. The Progression to Malignancy*; Humana Press: New York, 2006; p 678.

(38) Brochez, L.; Naeyaert, J. M. Serological markers for melanoma. *Br. J. Dermatol.* **2000**, *143* (2), 256–68.

(39) Chen, H.; Jia, W. D.; Li, J. S.; Wang, W.; Xu, G. L.; Ma, J. L.; Ren, W. H.; Ge, Y. S.; Yu, J. H.; Liu, W. B.; Zhang, C. H.; Wang, Y. C. Extracellular matrix protein 1, a novel prognostic factor, is associated with metastatic potential of hepatocellular carcinoma. *Med. Oncol.* **2010**, DOI: 10.1007/s12032-010-9763-1 .

(40) Baker, J. B.; Low, D. A.; Simmer, R. L.; Cunningham, D. D. Protease-nexin: a cellular component that links thrombin and plasminogen activator and mediates their binding to cells. *Cell* **1980**, *21* (1), 37–45.

(41) Xu, D.; McKee, C. M.; Cao, Y.; Ding, Y.; Kessler, B. M.; Muschel, R. J. Matrix metalloproteinase-9 regulates tumor cell invasion through cleavage of protease nexin-1. *Cancer Res.* **2010**, *70* (17), 6988–98.

(42) Yamashita, T.; Yoneta, A.; Hida, T. Macrophage inhibitory cytokine-1: a new player in melanoma development. *J. Invest. Dermatol.* **2009**, *129* (2), 262–4.

(43) Boyle, G. M.; Pedley, J.; Martyn, A. C.; Banducci, K. J.; Strutton, G. M.; Brown, D. A.; Breit, S. N.; Parsons, P. G. Macrophage inhibitory cytokine-1 is overexpressed in malignant melanoma and is associated with tumorigenicity. *J. Invest. Dermatol.* **2009**, *129* (2), 383–91.

(44) Mimeault, M.; Batra, S. K. Divergent molecular mechanisms underlying the pleiotropic functions of macrophage inhibitory cytokine-1 in cancer. *J. Cell. Physiol.* **2010**, *224* (3), 626–35.

(45) Ugurel, S.; Bell, N.; Sucker, A.; Zimpfer, A.; Rittgen, W.; Schadendorf, D. Tumor type M2 pyruvate kinase (TuM2-PK) as a novel plasma tumor marker in melanoma. *Int. J. Cancer* **2005**, *117* (5), 825–30.

(46) Guba, M.; Steinbauer, M.; Ruhland, V.; Schutz, A.; Geissler, E. K.; Anthuber, M.; Vogt, T.; Bosserhoff, A.; Jauch, K. W. Elevated MIA serum levels are predictors of poor prognosis after surgical resection of metastatic malignant melanoma. *Oncol. Rep.* **2002**, *9* (5), 981–4.

(47) Fukaya, Y.; Shimada, H.; Wang, L. C.; Zandi, E.; DeClerck, Y. A. Identification of galectin-3-binding protein as a factor secreted by tumor cells that stimulates interleukin-6 expression in the bone marrow stroma. *J. Biol. Chem.* **2008**, *283* (27), 18573–81.

(48) Kim, Y. S.; Jung, J. A.; Kim, H. J.; Ahn, Y. H.; Yoo, J. S.; Oh, S.; Cho, C.; Yoo, H. S.; Ko, J. H. Galectin-3 binding protein promotes cell motility in colon cancer by stimulating the shedding of protein tyrosine phosphatase kappa by proprotein convertase 5. *Biochem. Biophys. Res. Commun.* **2010**, *404* (1), 96–102.

(49) Gaggioli, C.; Robert, G.; Bertolotto, C.; Bailet, O.; Abbe, P.; Spadafora, A.; Bahadoran, P.; Ortonne, J. P.; Baron, V.; Ballotti, R.; Tartare-Deckert, S. Tumor-derived fibronectin is involved in melanoma cell invasion and regulated by V600E B-Raf signaling pathway. *J. Invest. Dermatol.* **2007**, *127* (2), 400–10.

(50) Prada, F.; Benedetti, L. G.; Bravo, A. I.; Alvarez, M. J.; Carbone, C.; Podhajcer, O. L. SPARC endogenous level, rather than fibroblast-produced SPARC or stroma reorganization induced by SPARC, is responsible for melanoma cell growth. *J. Invest. Dermatol.* **2007**, *127* (11), 2618–28.

(51) Fukunaga-Kalabis, M.; Santiago-Walker, A.; Herlyn, M. Matricellular proteins produced by melanocytes and melanomas: in search for functions. *Cancer Microenviron.* **2008**, *1* (1), 93–102.

(52) Fukunaga-Kalabis, M.; Herlyn, M. Unraveling mysteries of the multifunctional protein SPARC. *J. Invest. Dermatol.* **2007**, *127* (11), 2497–8.

(53) Podhajcer, O. L.; Benedetti, L. G.; Girotti, M. R.; Prada, F.; Salvatierra, E.; Llera, A. S. The role of the matricellular protein SPARC in the dynamic interaction between the tumor and the host. *Cancer Metastasis Rev.* **2008**, *27* (4), 691–705.

(54) Robert, G.; Gaggioli, C.; Bailet, O.; Chavey, C.; Abbe, P.; Aberdam, E.; Sabatie, E.; Cano, A.; Garcia de Herreros, A.; Ballotti, R.; Tartare-Deckert, S. SPARC represses E-cadherin and induces mesenchymal transition during melanoma development. *Cancer Res.* **2006**, *66* (15), 7516–23.

(55) Smit, D. J.; Gardiner, B. B.; Sturm, R. A. Osteonectin down-regulates E-cadherin, induces osteopontin and focal adhesion kinase activity stimulating an invasive melanoma phenotype. *Int. J. Cancer* **2007**, *121* (12), 2653–60.

(56) Denhardt, D. T.; Noda, M.; O'Regan, A. W.; Pavlin, D.; Berman, J. S. Osteopontin as a means to cope with environmental insults: regulation of inflammation, tissue remodeling, and cell survival. *J. Clin. Invest.* **2001**, *107* (9), 1055–61.

(57) Rangaswami, H.; Bulbule, A.; Kundu, G. C. Osteopontin: role in cell signaling and cancer progression. *Trends Cell. Biol.* **2006**, *16* (2), 79–87.

(58) Hayashi, C.; Rittling, S.; Hayata, T.; Amagasa, T.; Denhardt, D.; Ezura, Y.; Nakashima, K.; Noda, M. Serum osteopontin, an enhancer of tumor metastasis to bone, promotes B16 melanoma cell migration. *J. Cell. Biochem.* **2007**, *101* (4), 979–86.

(59) Sturm, R. A. Osteopontin in melanocytic lesions--a first step towards invasion? *J Invest. Dermatol.* **2005**, *124* (5), xiv–xv.

(60) Buback, F.; Renkl, A. C.; Schulz, G.; Weiss, J. M. Osteopontin and the skin: multiple emerging roles in cutaneous biology and pathology. *Exp. Dermatol.* **2009**, *18* (9), 750–9.

(61) Rangaswami, H.; Kundu, G. C. Osteopontin stimulates melanoma growth and lung metastasis through NIK/MEKK1-dependent MMP-9 activation pathways. *Oncol. Rep.* **2007**, *18* (4), 909–15.

(62) Packer, L.; Pavey, S.; Parker, A.; Stark, M.; Johansson, P.; Clarke, B.; Pollock, P.; Ringner, M.; Hayward, N. Osteopontin is a downstream effector of the PI3-kinase pathway in melanomas that is inversely correlated with functional PTEN. *Carcinogenesis* **2006**, *27* (9), 1778–86.

(63) Zhou, Y.; Dai, D. L.; Martinka, M.; Su, M.; Zhang, Y.; Campos, E. I.; Dorocicz, I.; Tang, L.; Huntsman, D.; Nelson, C.; Ho, V.; Li, G. Osteopontin expression correlates with melanoma invasion. *J. Invest. Dermatol.* **2005**, *124* (5), 1044–52.

(64) Meierjohann, S.; Schartl, M.; Volff, J. N. Genetic, biochemical and evolutionary facets of Xmrk-induced melanoma formation in the fish Xiphophorus. *Comp. Biochem. Physiol. C: Toxicol. Pharmacol.* **2004**, *138* (3), 281–9.

(65) McGary, E. C.; Lev, D. C.; Bar-Eli, M. Cellular adhesion pathways and metastatic potential of human melanoma. *Cancer Biol. Ther.* **2002**, *1* (5), 459–65.

(66) Maung, K.; Easty, D. J.; Hill, S. P.; Bennett, D. C. Requirement for focal adhesion kinase in tumor cell adhesion. *Oncogene* **1999**, *18* (48), 6824–8.

(67) Kahana, O.; Micksche, M.; Witz, I. P.; Yron, I. The focal adhesion kinase (P125FAK) is constitutively active in human malignant melanoma. *Oncogene* **2002**, *21* (25), 3969–77.